BE COATINGS ON SPHERICAL SURFACE FOR NIF TARGET DEVELOPMENT

H. Xu, A. Nikroo, J.R. Wall, R. Doerner,[†] M. Baldwin,[†] and J.H. Yu[†]
General Atomics, P.O. Box 85608, San Diego California 92186-5608, xuh@fusion.gat.com
[†]University of California, San Diego, 9500 Gilman Drive, La Jolla, California 92093

Beryllium is one of the preferred ablators for achieving ignition in inertial confinement fusion (ICF). Thin and thick coatings of Be on CH shells have been deposited using a sputter coater established at UCSD's PISCES facility and examined using a variety of characterization techniques. Due to the spherical nature of these substrates, shadowing effects are expected to play significant roles in film growth as well as the expected surface diffusion length of deposited atoms. Be coatings on flat surfaces and spherical surfaces have been deposited and compared to understand the material growth behaviors on different surfaces and as a function of processing parameters. On flat surfaces, Be film developed polycrystalline morphology with columnar growth. On spherical surfaces, Be film also showed columnar growth at lower powers, which then transitioned into a twisted grain structure at higher powers. Cycling of parameters has been used to investigate possible grain growth interruption during growth and improving morphology. Initial results also suggest that copper doping during deposition does not change the columnar growth morphology. Measurements of the surface roughness of beryllium-coated shells indicate roughness growth proportional to the thickness with an exponent of 0.8 to 1.2, which is consistent with shadowing dominated roughening. As ion-beam-assisted growth may improve the surface finish and micro-structure of deposited films, we have also studied the effect of process parameters on the flux and energy of the ions reaching the substrates using an offline energy dispersive mass spectrometer system.

I. INTRODUCTION

Beryllium is one of the preferred ablators for achieving ignition on the National Ignition Facility (NIF) because of its high density, low opacity, high tensile strength and high thermal conductivity.[1]

Sputter coating of beryllium on plastic mandrels is one possible means of producing beryllium shells for NIF. It has been investigated for some time and Be coatings on spherical polymer mandrels have been demonstrated.[2–5] It is potentially the only technique that would allow a graded copper doped ablator as is currently proposed for NIF due to its superior stability during implosion. However, due to the directional nature of the sputter coating process and low temperature limitation of plastic mandrels, such coatings can suffer from low density and high defect density. The coating surface roughness also generally increases with film thickness. A better understanding of coated Be film density, the development of void defects in the film and how they are affected by surface roughness will help to develop strategies for improving film qualities. Although a number of modifications to the baseline coating process have been investigated to improve the coating quality in the past, such as addition of a bias to the substrates or incorporating impurities, etc. there is still a gap in meeting NIF specifications. In this effort, we have investigated several issues related to the coatings and the parameters used in order to obtain a better understanding of the process. These include the evolution of surface roughness with coating thickness to determine the effects of self-shadowing due to the spherical nature of the substrates, the effect of coating rate on micro-structure of the coatings, as well examining possible effects due to doping of the coatings with copper. In addition, as ion bombardment is often used in sputtering to increase film density, we have also investigated the effects of the process parameters on flux and energy of ions emitted from a commercial ion source (Oxford Scientific OSPREY ion source). This work has been performed in a beryllium coater established in the dedicated beryllium certified enclosure at UCSD's energy research center which has extensive ventilation to prevent the potential respiratory diseases associated with Be particles. In this preliminary work only coating thicknesses of approximately ≤50 μm were examined for the most part, compared to a required thickness of ~150 μm for NIF targets. Further experiments will deal with thicker films.

II. EXPERIMENTS

Our coating experiments were performed in a high vacuum chamber equipped with three 5 cm diameter Be magnetron sputter source and one 5 cm diameter Cu magnetron sputter source. The system is evacuated to a base pressure of $\sim 1\times10^{-6}$ Torr after over night pumping. The sputtering gas is high purity Ar (99.999%). Coating

normally was performed on 2 mm diameter CH mandrels (20–30 μm in thickness) agitated in a bounce pan attached to an electromagnetic shaker driven by a sound amplifier. The coating normally was done at 3–10 mTorr of Ar gas pressure. The Be targets to bounce pan distance was set to be ~10 cm. The Cu target to bounce pan distance can be adjusted to achieve desired doping levels. The coating process was monitored through a window by a video camera. The thickness of the Be coating on CH mandrel was measured by SEM and x-ray radiography and used to calibrate the coating rate. The power applied to the Be sputter targets ranged from 100 to 200 W. Be sputter source power was cycled at regular intervals in some runs from 100 to 200 W during Be coating. Typical coating rate for three Be guns at 100 W is 0.4–0.5 μm/h. A 50 μm Be film will take ~5 days continuous coating. Cu doped layers were produced by using the Cu source (at <10 W) in addition to the Be sputtering. The Cu gun power and distance was changed to obtain coatings with Cu content of <1 to ~3 at. %.

Coatings were characterized using a variety of techniques to examine coating structure, roughness, density and composition. The microstructure was examined by SEM. Surface roughness RMS data was obtained by using the AFM spheremapper. Be film density was measured using two methods. The first method is based on using the ratio of the measured mass and volume of the shells. Shells were weighed using a Conn microbalance accurate to 0.3 μg. Since the weight of the beryllium coated shells is typically ~2 mg or higher, the error in density due to weighing is well below 0.1%. The accuracy of diameter measurements using x-ray radiography is ~1 μm, introducing an error of ~only 0.1% in the density measurements. The thickness measurement contributes the most error to the density measurements. The thickness is typically measured using radiography which can have an error of as much as 2 μm, with the associated error of 4% in the density. Therefore, the error in density measurement is about 4% currently, although there is a focused effort to reduce this error. The second method is a liquid floating measurement. By mixing a low density and a high density fluid, a variable density fluid can be produced. When the correct mixture of the two fluids is used, a shard from Be coated shell would float in the mixture. Using a densitometer accurate to greater than 0.01 g/cc to measure the density of the mixture, allows determination of the coating density to that accuracy (<1%). However, this technique requires the removal of CH mandrel first by heating in an oven at 500°C for 40 h. This heat treatment introduces uncertainties in the density of the coating as there may be slight oxidation in the Be coating during mandrel removal which can increase the density and lead to an artificially high density for the coating. Nonetheless, this measurement was also used as a consistency check.

Cu concentration was measured by electron probe microanalysis (EPMA), x-ray fluorescence (XRF) and x-ray radiograph modeling. Each method has an accuracy of 10%–20%. It seems that there are some discrepancies in Cu concentration measured by different methods. To get better accuracy it may be necessary to measure a standard Cu doped sample by different tools to resolve the differences.

III. RESULTS

We initially prepared numerous 50 μm Be coatings on CH mandrels at 100 W of power to the three Be sources to examine the reproducibility of the process. Fracture cross sections of coatings were examined in the SEM to examine the microstructure. It is seen from Fig. 1(a) that the fracture cross section of a ~50 μm coating on a capsule indicates columnar texture of the Be capsule throughout coating. This type of structure was consistently seen when growing at the coating rate of ~0.5 μm/h typical of deposition at 100 W for the three guns. For comparison purposes, a SEM cross-section of Be coating on a flat surface is shown in Fig. 1(b). Similar columnar texture is also observed. This suggests that

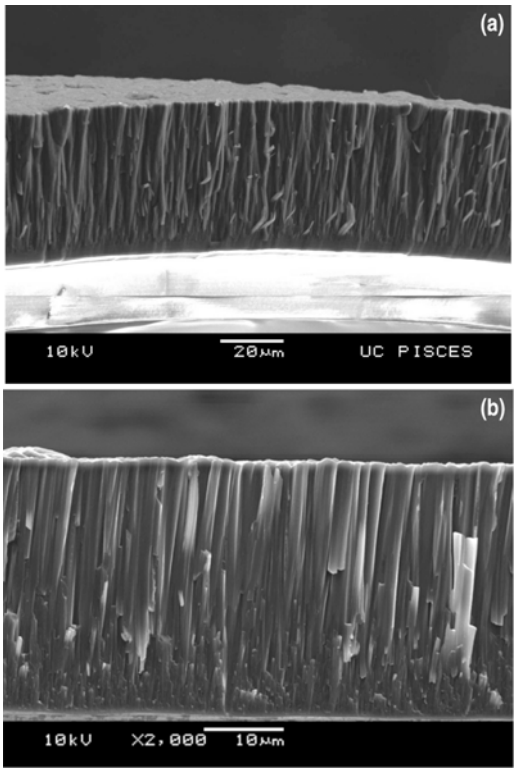

Fig. 1. (a) A cross-section SEM image of a ~50 μm Be shell showing consistent columnar structure. (b) A cross-section SEM picture of a Be coating on a flat Si substrate, which also shows columnar grain growth.

columnar texture is a common structure of magnetron sputtering independent of the substrate shape. Measurements of the temperature of the bounce pan indicate a temperature of ~130°–150°C during Be coating. This corresponds to a temperature of that is ~0.25 of the melting temperature of the beryllium metal agreeing with the expected structure from the zone T growth from Thornton's structure zone model (SZM).[6]

The surface roughness information is useful in identifying film surface roughening mechanism. Normally as coating thickness increases, the film surface becomes rougher. The surface roughness RMS versus film thickness follows a power law, $R \sim d^{\beta}$, R is surface roughness RMS, d is film thickness and β is a power component.[7] Roughness in the surface is related to rough internal interfaces and may introduce more defects in the film. To understand coating surface roughening mechanisms, we investigated the film roughness versus film thickness by AFM. Figure 2 shows an AFM power spectrum of a typical capsule surface. AFM was scanned along the equators of the spheres and the traces were converted to power spectra by Fourier transforms. The high mode (m > 100) RMS represents surface roughness. The plot shows a surface roughness RMS (101–1000) of 282 nm for a ~50 μm

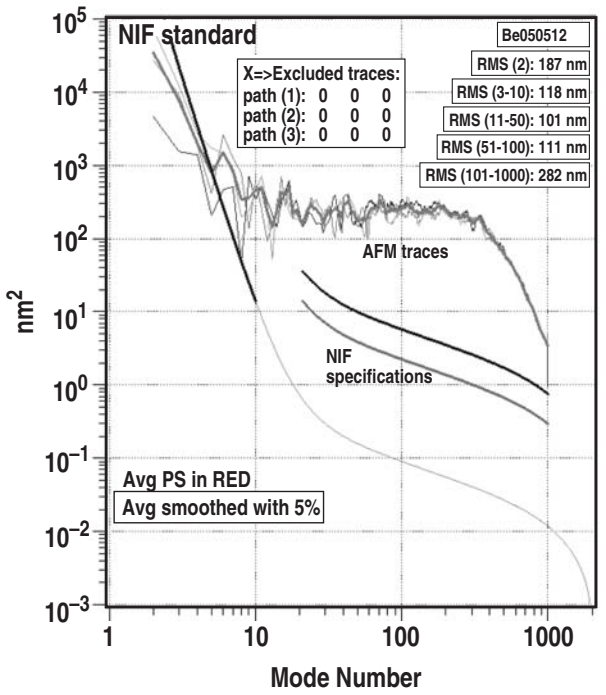

Fig. 2. A typical AFM spheremapping power spectrum of a ~50 μm Be coating on a 2 mm CH mandrel. The smooth lines are NIF specifications for Be capsules. The upper curves are from AFM traces on the sphere surface.

coating. Figure 3 shows plots of film surface roughness high mode RMS versus film thickness for two groups of samples. The first group samples, which was prepared at 10 mTorr, with 3–6 shells in each batch, and bounced at 120 Hz ~0.9 V bias showed a power exponent of $\beta \sim 0.78$. The other group of samples, which were prepared at 10 mTorr, with 12–15 shells in each batch, and bounced at ~110 Hz and up to 1.9 V bias. The power component for this group of samples is 1.19. These roughness power components are higher than those normally observed on flat surfaces, which are typically <0.5–0.6.[7]

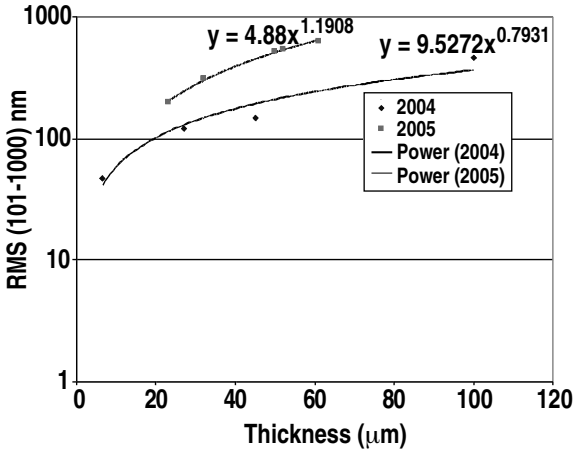

Fig. 3. A plot of high mode surface roughness RMS versus film thickness. Two groups of samples give RMS component from 0.78 to 1.19.

According to a ballistic deposition model, the exponent will have a value of 1/3 at small angles of incidence (near normal) and increases with incident angle to approach 1/2 for large angles.[8] Considering the shadowing effect, which describes how high spots shadow low spots on a surface and is more pronounced at off-normal incidence, the value increased to ~0.7–1.0 depending on incident flux angle distribution.[9] The value of RMS roughness component of our coatings on spherical surface is consistent with shadowing dominated mechanism. Since our coating is on spherical mandrels, an incident flux is at an angle to a surface normal, which changes from the middle of the mandrel surface to the edge. The large angles near the edge of mandrel surface lead to stronger shadowing effect and fast roughening behavior. This could be the reason for our observation of faster growth of the RMS power exponents.

One of the important parameters for NIF target is the sputtered Be film density. Measurements from metrology and floating give similar results. Table I showed a few measurements of Be coating density by two methods. Since Be bulk density is 1.847 g/cc, our measurements of

the density by first method suggest that Be coating is ~95%–96% of the bulk density after deposition assuming no contamination. Although the measurements have an accuracy of ±3%, it is still encouraging that sputtered Be film showed near full density. Our recent TEM observations indicate existence of low density and small size voids in the sputter coated Be films, which is consistent with less than full density Be films. The second method gives a slightly higher density, which can be explained by some surface oxidation during annealing. These data suggest that the coated Be film density is fairly high. However, the measurements here are limited to coatings of ≤50 μm thickness.

TABLE I. Density Measurements of Be Coatings

ρ = m/V Measurements	
Be Shells	Density (g/cc)(±3%)
Be050325, 49 μm	1.74
Be050408, 55 μm	1.76
Be050509, 44 μm	1.76
Be050420, 53 μm	1.74
Buoyant Force Measurements	
Be Shells	Density (g/cc)±0.01 g/cc
Be050325, 49 μm	1.84
Be050408, 53 μm	1.84
Be050215, 23 μm	1.85

Be coatings doped with Cu and also multi-layer graded Cu-doped Be coatings were produced by co-sputtering of Be and Cu targets. As seen from a backscattering image in Fig. 4(a), layered structure can be seen with different contrasts which represent different Cu doping levels. The darker area indicates lower Cu doping level. E-probe measurement and x-ray radiograph modeling suggest the heavier Cu doped layer has a Cu concentration of ~1.7%–1.9%. The lighter Cu doped layer has a Cu concentration of 1.1%. The SEM image [Fig. 4(b)] shows a columnar structure, which is continuous from Be layer to Cu doped layers. This suggests that Cu doping does not change the nature of columnar growth of Be films even at these higher doping levels. Coatings with as low as 0.35 at. % and as high as ~3 at. % Cu were produced.

Another important observation is micro-particle incorporation into the coating. Figure 5(a) shows a SEM picture of a cross section of a Be/Be(Cu) coated shell. It is seen that micro-particle initiated growth embeds in the film. By measuring the height and the width of the "cone-shaped" grain, it is noticed that the width and height of the features roughly follow square root relation. The micro-particles seem to embed in the film and start as new growth center as evidenced by the disruption of normal columnar growth pattern. The particle initiated growth could start from any stage of the film growth suggesting

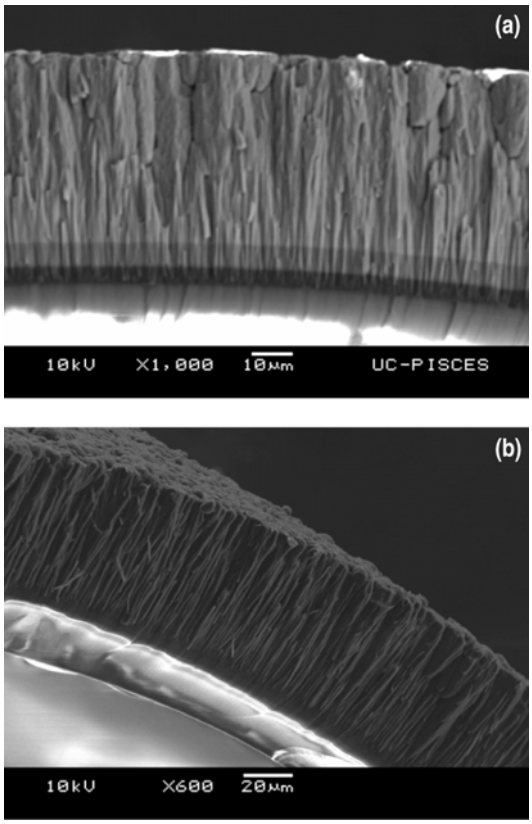

Fig. 4. (a) A backscattering image of graded Cu doped Be multilayer structure showing different contrast from pure Be layer to lightly doped Be layer and heavily doped Be layer. (b) A SEM picture of the same Be multilayer structure shows continuous columnar grain growth.

that they incorporated into the film during film growth. The incorporation of particles in the film can have significant effects on surface roughness and induce growth defects. The micro-particles landing on the surface of the coating induce extra roughness, which can cause fast roughening by shadowing effects. Figure 5(b) is a corresponding power spectrum of Figure 5(a) shell. The high mode surface roughness RMS of Fig. 5(b) is 523 nm, which is much higher than the typical 280 nm RMS observed in Fig. 2. This suggests that micro-particle incorporation leads to rougher surface. The origin of those particulates during growth is not clear. However, there are a few possible ways the micro-particles can be generated. During the coating process, the spherical CH mandrels are agitated by a bouncing pan. The collision between shells presumably can cause some coating material chipped off, which can be a source of particulates. If that is the case, the effect will be enhanced with weight increasing. Our observation seems to indicate that at earlier stage of the coating process, the bouncing pan is shining and clean. Some dusts or debris normally can be seen in the bouncing pan after a few days' coating. Another source of particulate could come from the surrounding of the

magnetron guns. Thick Be coatings normally accumulated around the anode shield after extended coating. Strong plasma near the gun during coating process could also sputter off some materials from surrounding shield and generate some particulates. In the surface roughness RMS data presented in Fig. 3, it seems that the RMS component for a group of samples coated in 2004 when the coater was first used is smaller, which suggests that more particulates are generated after extended use of the coater and larger RMS components for samples coated in 2005 may be attributed to particulate enhanced roughness. Further experiments are necessary to identify the origin of those sources.

The coating shown in Fig. 6 showed a transition to twisted columnar texture near the top of the coated film, which corresponds to a sputter power change from 100 W to 150 W. This structure has been examined extensively recently and has the undesirable feature of having a very low density (~1.5 g/cc).[10] This change of orientation of the fiber column has been observed previously in sputtered films when the power or pressure changes. They were attributed to energetic particle preferential sputtering effect.[11] Coating at higher power is in general desirable as it allows coating at a higher rate and therefore a faster shell fabrication process. However, low density is not desired. In order to avoid the undesirable transition to the low density twisted structure while still achieving a higher coating rate when the power level was changed, we used cycling of Be source power levels during the coating. We also hoped that this would create a multilayer structure and show the multilayer smoothing effect. It has been demonstrated in a recent work of planarizing reticle substrates for extreme ultraviolet lithography very smooth surface finish has been achieved by using Mo-Si multilayers.[12–13] It was also found that using multilayers of Si/Mo or ion etching of Si layers in between deposition of Si/Mo multilayers, extremely smooth surface can be achieved, albeit for very thin layers (<1 μm). Another recent work showed that alternating substrate biasing during film growth produced a laminate structure with alternating layers of distinctly different microstructure.[14] Our results on different thickness of layers indicate while there was no evidence that the film surface becomes smoother with cycling of the power by AFM measurements, the cycling of the power consistently suppressed the twisted structure.

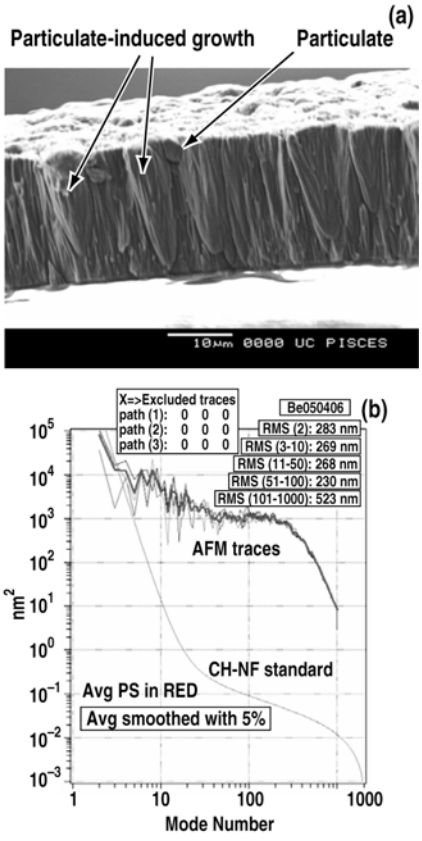

Fig. 5. (a) shows a SEM cross section picture of a Be coated shell. Some particulate induced growth can be seen in (a), indicated by growth pattern change from normal columnar grain growth. (b) is a corresponding sphere-mapping power spectra of (a).

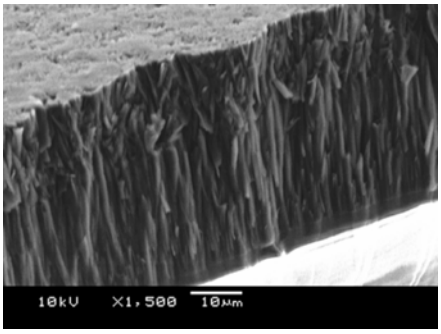

Fig. 6. A SEM cross section of a Be coating which showed a transition to twisted columnar structure near top of the coated film. The transition corresponds to a sputter power change from 100 W to 150 W.

IV. DISCUSSION

While the densities obtained in this work are only several percent lower than that of full density beryllium, we discuss several possible ways of increasing density in future work. Surface roughening behavior may have important impact to the material density, void density and surface/interface roughness. It has been shown that film growth experiences short-range smoothening due to diffusion and global roughening due to self-shadowing.[15] Simulations suggest that columnar texture is a common

structure of film growth caused by self-shadowing effects. The shadowing effect depends on incident atom flux angles. The orientation of grain columns, the porosity, the crystallographic texture, and grain sizes are sensitive to the deposition angles.[16] High porosity is shown at larger angles. The mean void size increases with film thickness and incident angles. It has been proposed that biased diffusion can suppress self-shadowing effect.[16] Biased diffusion occurs when an arriving atom does not lose all of its kinetic energy in the first collision with a surface atom and uses the remaining in-plane momentum to move over the surface. It has been shown that at low energy (<5 eV) and off-normal incidence, shadowing is dominated. Defects tend to become larger as the film evolves, leading to a voidy, rough film. At higher energy (3–20 eV) and off-normal incidence, biased diffusion is found to be dominant. The shadowing is suppressed on the nanoscale, and the defects are filled as the film grows. This could lead to dense and smooth films.

In a magnetron sputtering system, atoms leave the target with a so-called Sigmund-Thompson distribution, which implies a kinetic energy of a few electron volts depending on target material binding energy and atomic mass. This energy will be further reduced by the gas phase scattering during transport to the substrate. The simplest way to preserve atom energy is to reduce the carrier gas pressure and target substrate distance. Another approach is to generate a mostly ionized target beam flux by high-power pulsed magnetron sputtering (HPPMS) and to accelerate the ions to the substrate by a biasing. It has been demonstrated that a smooth and dense Ta film was fabricated in this way.[17]

Ion beam assisted deposition is another option to get smooth and dense film. Although Ar ions are not as effective as target material ions to enhance mobility on the surface, improved material quality can still be achieved by tuning ion energy and ion-to-atom ratio.[18–19] Due to shadowing effects, ion beam can also smooth the surface by removing the irregularity on the surface. As demonstrated in the literature, deposition/ion etching cycles achieved better surface finish.[11–12] Since NIF target requires very thick coatings (up to 170 μm) of Be and Be(Cu) on spherical surfaces, it is important to control surface roughness because the surface roughness is expected to grow with thickness due to the power scaling law. While polishing of shells can reduce surface roughness, the improvements in the surface roughness due to surface mobility enhancement of adatoms and ion beam etching could potentially help to reach the goal of smooth and dense coatings.

To understand the effectiveness of ion beam, we performed some measurements by Mass Spectrometry to determine the ion beam flux changes with distance and Ar gas pressures. This is important, as ion beam bombardment in the sputter chamber will involve loss of ion flux and energy in transport from the ion gun to the substrates. The setup of the measurement is shown in Fig. 7. An Oxford Scientific OSPrey plasma ion source was used to generate broad beam low energy ions. The Ar ion beam interacts with Ar neutrals in the vacuum chamber, and undergoes elastic scattering and charge exchange. Ions that are directed on-axis then enter the quadruple mass spectrometer (QMS) through a small (50 or 500 μm) orifice. The QMS has a 45 deg. electrostatic energy filter and a set of four dc- and ac-biased rods that allow passage of ions with a particular charge-to-mass ratio.

Figure 8 shows a plot of energy scan at various distances (a) and the measured ion current density versus distances (b). The ion energy is determined by the anode voltage and plasma potential. The ion current density

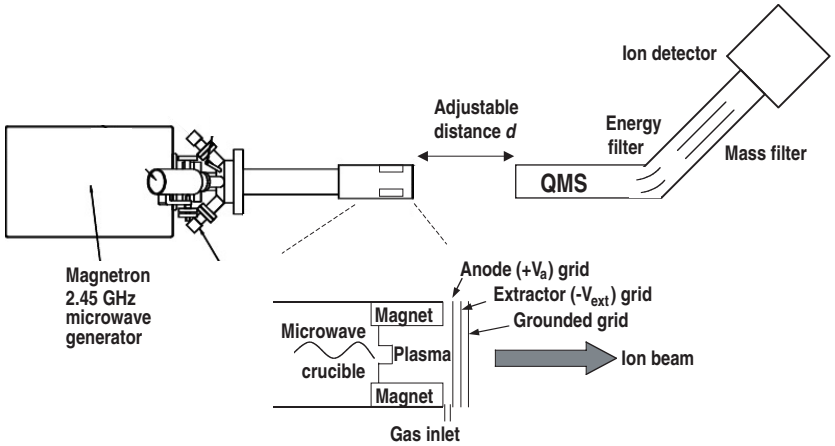

Fig. 7. A schematic setup of ion beam measurement by QMS.

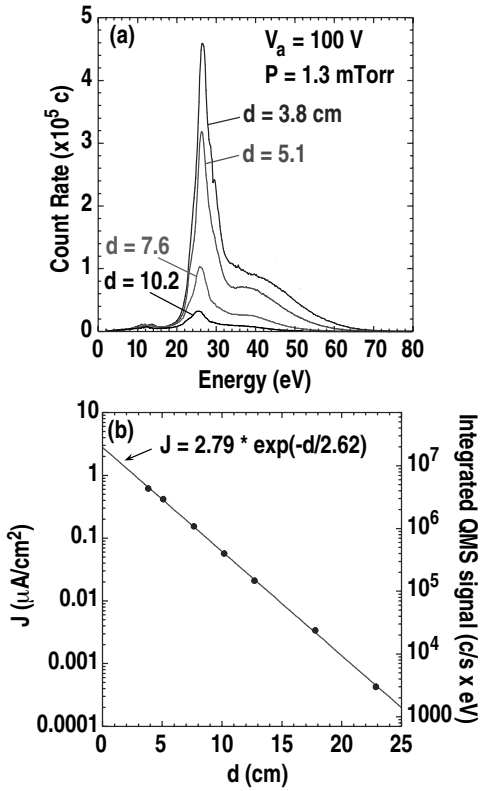

Fig. 8. (a) Energy scans of an ion beam at different distances. (b) A plot of ion current density versus distance.

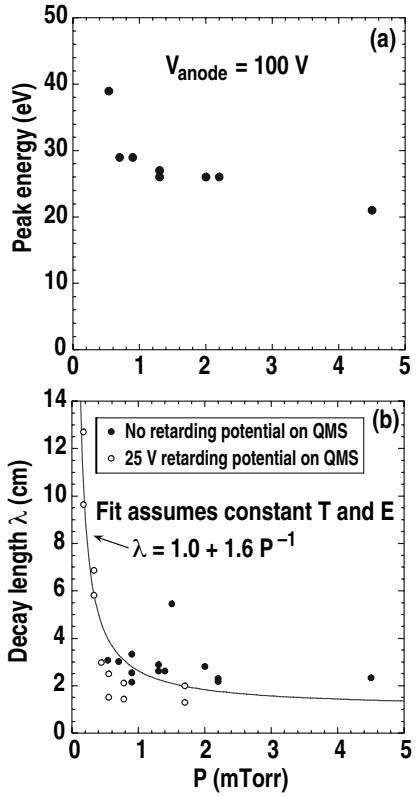

Fig. 9. (a) A measure of ion energy peak position versus Ar pressure. (b) A plot of ion current decay length versus Ar pressure for the measured beam. T and E are gas temperature and ion energy, respectively.

decays exponentially with distance. A fitting to an exponential function gives a decay length. Figure 9 shows the measured peak energy positions with Ar pressures (a) and the decay length versus Ar pressures. It is clear from the plot that Ar ion decay length at typical sputtering condition is very short (<2.54 cm). The energy of the ions also drifted lower with increasing Ar pressure. This indicates that Ar pressure and ion gun to substrate distance is critical in determining the effectiveness of the ion beam transport to the substrates and the resulting film quality.

V. SUMMARY

Be coatings on CH mandrels have been prepared and initial characterization indicates the films with thickness <50 μm can be produced at ~0.5 μm/h with consistent columnar structure that have densities within several percent of bulk Be density. The surface roughness of the coatings has been studied to identify the roughening mechanism. The roughness RMS growth exponent of 0.8–1.2 of the films suggests that self-shadowing is one of the dominant roughening mechanisms. Coatings at higher powers lead to a transition to an undesirable low density twisted structure. This structure can be avoided while coating at a higher rate by cycling the power to sputter sources (cycling coating rate). Micro-particle, generated during coating by either shell agitation or sputter source debris, incorporation appears to be a major contribution to fast film roughening. Cu doped films have been made with doping levels of ~0.5 to 3 at. %. Cu doping does not appear to affect the evolution of the film microstructure. Some possible ways of suppressing the self-shadowing effect and improving film density further for thick films are proposed.

ACKNOWLEDGMENTS

Work supported by the U.S. Department of Energy under Contract No DE-AC03-01SF22260. The authors acknowledge J.B. Gibson for providing AFM spheremapping measurements, M. West for providing mandrel removed sample for density measurements, H. Huang and S. Eddinger for providing x-ray radiograph diameter measurements, M.L. Hoppe for performing the buoyant force measurements and R. Paguio for providing densitometer measurements, and C. Alford, M. McElfresh and R.C. Cook of LLNL for useful comments and discussions.

REFERENCES

1. D.C. WILSON, P.A. BRADLEY, N.M. HOFFMAN, F.J. SWENSON, D.P. SMITHERMAN, R.E. CHRIEN, R.W. MARGEVICIUS, D.J. THOMA, L.R. ROREMAN, J.K. HOFFER, S.R. GOLDMAN, S.E. CALDWELL, T.R. DITTRICH, S.W. HAAN, M.M. MARINAK, S.M. POLLAINE, and J.J. SANCHEZ, "The Development and Advantages of Beryllium Capsules for the National Ignition Facility," *Phys. Plasmas* **5**, 1953 (1998).
2. R.J. BURT, S.F. MEYER, and E.J. HSIEH, "Radio Frequency Magnetron Sputtering of Thick Film Amorphous Beryllium," *J. Vac. Sci. Technol.* **17**, 407 (1980).
3. E.J. HSIEH, C.W. PRICE, E.L. PIERCE, and R.G. WIRTENSON, *J. Vac. Sci. Technol.* **A 8**, 2165 (1990).
4. R. McEACHERN, C. ALFORD, R. COOK, D. MAKOWCKI, and R. WALLACE, "Sputter-Deposited Be Ablators for NIF Target Capsules," *Fusion Technol.* **31**, 435 (1997).
5. R. McEACHERN and C. ALFORD, "Evaluation of Boron-Doped Beryllium as an Ablator for NIF Target Capsules," *Fusion Technol.* **35**, 115 (1999).
6. J.A. THORNTON, "The Microstructure of Sputter-Deposited Coatings," *J. Vac. Sci. Technol.* **A4**, 3059 (1986).
7. A.E. LITA and J.E. SANCHEZ, JR., "Characterization of Surface Structure in Sputtered Al Films: Correlation to Microstructure Evolution," *J. Applied Phys.* **85**, 876 (1999).
8. P. MEAKIN, "Ballistic Deposition onto Inclined Surface," *Phys. Rev. A* **38**, 994 (1988).
9. J. YU and J.G. AMAR, "Dynamical Scaling Behavior in Two Dimensional Ballistic Deposition With Shadowing," *Phys. Rev. E* **66**, 21603 (2002).
10. MC ELFRESH *et al.*, "Sputtering Deposition Beryllium Capsules for NIF: a Progress Report," these proceedings.
11. J.M.E. HARPER and K.P. RODBELL, "Microstructure Control in Semiconductor Metallization," *J. Vac. Sci. Technol.* **B15**, 763 (1997).
12. P.B. MIRKARIMI, E. SPILLER, S.L. BAKER, V. SPERRY, D.G. STEARNS, E.M. GULLIKSON, "Developing a Viable Multilayer Coating Process for Extreme Ultraviolet Lithography Reticles," *J. Microlith., Microfab., Microsyst.* **3**, 139 (2004).
13. P.B. MIRKARIMI, E.A. SPILLER, D.G. STEARNS, V. SPERRY, and S.L. BAKER, "An Ion-assisted Mo-Si Deposition Process for Planarizing Reticle Substrates for Extreme Ultraviolet Lithography," *IEEE J. Quantum Electronics* **37**, 1514 (2001).
14. D.E. RUDDELL, B.R. STONER and J.Y. THOMPSON, "Effect of Deposition Interruption and Substrate Bias on the Structure of Sputter-Deposited Yttria-Stabilized Zirconia Thin Films," *J. Vac. Sci. Technol.* **A20**, 1744 (2002).
15. B.A. SPERLING and J.R. ABELSON, *Appl. Phys. Lett.* **85**, 3456 (2004).
16. PARITOSH and D.J. SROLOVITZ, "Shadowing Effects on the Microstructure of Obliquely Deposited Films," *J. Applied Phys.* **91**, 1963 (2002).
17. J. ALAMI, P.O.A. PERSSON, D. MUSIC, J.T. GUDMUNDSSON, J. BOHLMARK and U. HELMERSSON, "Ion-assisted Physical Vapor Deposition for Enhanced Film Pro*perties on Nonflat Surfaces,"* J. Vac. Sci. Technol. **A23,** 278 (2005).
18. I. PETROV, P.B. BARNA, L. HULTMAN, and J.E. GREENE, "Microstructural Evolution During Film Growth," *J. Vac. Sci. Technol.* **A21**, S117 (2003).
19. J.D. TORRE, G.H. GILMER, D.L. WINDT, R. KALYANARAMAN, F.H. BAUMANN, P.L. O'SULLIVAN, J. SAPJETA, T.D. RUBIA, M.D. ROUHANI, "Microstructure of Thin Tantalum Films Sputtered onto Inclined Substrates: Experiments and Atomistic Simulations," *J. Appl. Phys.* **94**, 263 (2003).